

Investigation of flux creep in high- T_c superconductors using Hall-sensor array

Y. Abulafia, D. Giller, Y. Wolfus, A. Shaulov, and Y. Yeshurun
Institute of Superconductivity, Department of Physics, Bar-Ilan University, Ramat Gan 52900, Israel

D. Majer and E. Zeldov
Department of Condensed Matter Physics, The Weizmann Institute of Science, Rehovot 76100, Israel

J. L. Peng and R. L. Greene
Department of Physics and Center for Superconductivity Research, University of Maryland, College Park, Maryland 20742

The details of a new method for studying thermally activated flux creep in thin superconducting samples is described. The method employs a linear array of microscopic Hall sensors to measure the time and spatial dependence of the magnetic induction across the sample. These data are analyzed on the basis of the local rate equation for thermally activated flux motion, taking into account both the in-plane and out-of-plane components of the induction field. Following this analysis, flux creep parameters, such as the flux-line current density, flux-line average velocity, and the activation energy for flux creep, can be directly determined as a function of position and time. New experimental data in a superconducting $\text{Nd}_{1.85}\text{Ce}_{0.15}\text{CuO}_{4-\delta}$ crystal demonstrate this method.
 © 1997 American Institute of Physics. [S0021-8979(97)18708-4]

Thermally activated flux creep in high-temperature superconductors has been the subject of many studies.^{1,2} This phenomenon is commonly investigated by measuring the time decay of the magnetic moment M averaged over the sample volume, using, for example, a vibrating sample magnetometer or a magnetometer based on a SQUID. In interpreting such data, one should realize that the behavior of the average magnetic moment is determined by the flux-line current density *at the sample surface*, where flux lines enter or exit the sample. Thus, such experiments yield information on the flux entry or flux exit process, but provide no direct information on the flux creep process within the sample. We have recently described a novel experimental technique for studying flux creep within the sample utilizing Hall-sensor arrays that allow measurements of the time evolution of the *local* induction B within the sample.³⁻⁵ This unique method yields a detailed picture of the relaxation process within the superconductor, including data on the flux line current density, the flux line average velocity, and the activation energy for flux creep, as a function of position and time. In this article, we further develop this method for a thin platelet sample, and demonstrate its capability by presenting new data on flux creep parameters in a $\text{Nd}_{1.85}\text{Ce}_{0.15}\text{CuO}_{4-\delta}$ (NCCO) crystal. A detailed study of the global magnetic properties of this NCCO system is described in Ref. 6. A complete study of its *local* magnetic properties, including investigation of the ‘‘fishtail’’ effect, will be described elsewhere.⁷ The NCCO crystal used in our study is approximately 20 μm thick with a relatively large aspect ratio (width/thickness) of approximately 17. As a result, both components of the induction field, perpendicular and parallel to the sample surface, play a role in the relaxation process. Our choice of a sample of such geometry serves the purpose of illustrating how the contributions of both components can be taken into account in the data analysis.

The differential equation governing flux creep in superconductors is derived from the Maxwell equation,

$\nabla \times \mathbf{E} = -(1/c)\partial\mathbf{B}/\partial t$ and the equation relating the electric field \mathbf{E} to the flux motion, $\mathbf{E} = (1/c)\mathbf{B} \times \mathbf{v}$, where \mathbf{v} is the average velocity of the vortices in the direction of the Lorentz force. These equations lead to

$$\partial\mathbf{B}/\partial t = -\nabla \times (\mathbf{B} \times \mathbf{v}). \quad (1)$$

We consider a rectangular sample of width much smaller than its length (along the y direction) and approximate it as an infinitely long strip with current flowing along its length, $\mathbf{j} = [0, j\text{sgn}(x), 0]$. For such a strip in a perpendicular field (parallel to the z axis), $\mathbf{B} = (B_x, 0, B_z)$, $\mathbf{v} = (v_x, 0, v_z)$, and Eq. (1) yields:

$$\frac{\partial B_z}{\partial t} = -\frac{\partial}{\partial x}(B_z v_x - B_x v_z), \quad (2)$$

$$\frac{\partial B_x}{\partial t} = -\frac{\partial}{\partial z}(B_x v_z - B_z v_x). \quad (3)$$

These two equations indicate that both components, B_z and B_x , exhibit relaxation, and that the relaxation of each component is *coupled* to that of the other. Since \mathbf{v} is in the direction of the Lorentz force which is perpendicular to \mathbf{B} , $\mathbf{v} \cdot \mathbf{B} = 0$, and Eqs. (2) and (3) become

$$\frac{\partial B_z}{\partial t} = -\frac{\partial}{\partial x}(Bv); \quad \frac{\partial B_x}{\partial t} = \frac{\partial}{\partial z}(Bv), \quad (4)$$

where $v = \sqrt{v_x^2 + v_z^2}$ and $B = \sqrt{B_x^2 + B_z^2}$ are the magnitude of the velocity \mathbf{v} and the induction \mathbf{B} .

Assuming thermal activation over the pinning barrier $U(j)$,

$$v = v_0 \exp(-U/kT), \quad (5)$$

where $v_0 = Aj\phi_0/c\eta$, ϕ_0 is the unit flux, c the light velocity, j the current density, η the viscosity coefficient, and A is a numerical factor^{3,8} of order 1. We calculate η using the

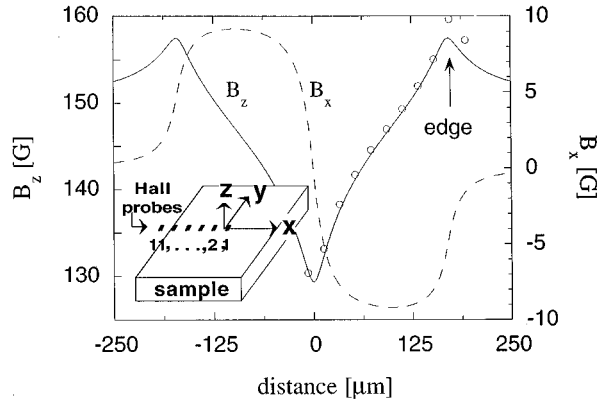


FIG. 1. Components B_z and B_x of the local induction in a NCCO crystal at 19 K, 30 s after applying a field of 150 G, described as a function of the distance from the center. Circles describe the measure data points. The solid line is a fit to a Bean-type model for B_z in a flat sample. The dashed line is the calculated B_x based on this fit. Inset: configuration of Hall-sensor array relative to the crystal.

Bardeen–Stephen formula $\eta = H_{c2} \phi_0 / \rho_n c^2$ (H_{c2} is the upper critical field and ρ_n is the normal resistivity) and the parameters given in Ref. 9.

In the experiment, we measure $B_z(x, t)$ which has contributions from the external field H and the current flowing in the bulk of the sample. For the sake of simplicity, and without affecting the generality of the analysis below, we assume here a constant j . The Biot–Savart law then implies $B_z \equiv H + (jd/c)G_z(x, z)$, where d is the thickness of the sample and $G_z(x, z)$ is a dimensionless geometrical factor which can readily be calculated.⁵ Thus, a one parameter fit to the B_z data yields j . The component B_x has a contribution only from the current density j . Once j is known, B_x and thus $B = \sqrt{B_x^2 + B_z^2}$ can be calculated.

The procedure of the data analysis is as follows: We first spatially integrate the measured values of $\partial B_z / \partial t$ to obtain the flux line current density $D \equiv Bv$. Knowing $D(x, t)$ and B , we determine $v = D/B$ from Eq. (4). The activation energy $U(x, t)$ is then derived by using Eq. (5):

$$U(x, t) = kT \ln\left(\frac{v_0}{v}\right). \quad (6)$$

Following the above procedure, measurements of $B_z(x, t)$ enable direct determination of $D(x, t)$, $v(x, t)$, and $U(x, t)$.

Measurements were performed on a $\text{Nd}_{1.85}\text{Ce}_{0.15}\text{CuO}_{4-\delta}$ crystal ($T_c \approx 22$ K) with dimensions $1.2 \times 0.35 \times 0.02$ mm³, which was grown using a directional solidification technique.¹⁰ An array of 11 Hall sensors with sensitivity better than 0.1 G, made of GaAs/AlGaAs (2DEG), was in a direct contact with the surface of the crystal, as sketched in the inset to Fig. 1. The active area of each sensor was 10×10 μm². The sensors detect the component B_z of the field normal to the surface of the crystal. In the following, we present data taken in the presence of a field of 150 G which was applied at 19 K after a zero-field-cooling process.

Figure 1 displays typical field profiles $B_z(x)$ across the sample width measured 30 s after application of the field. The solid line in this figure is calculated on the basis of a

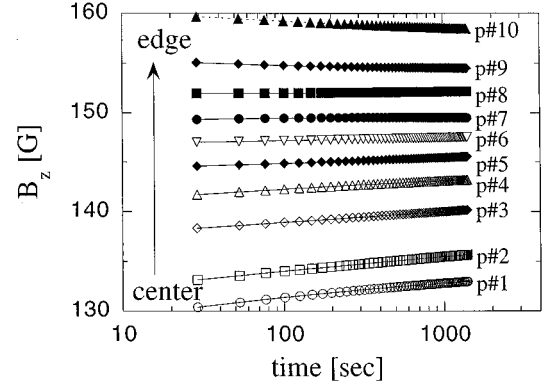


FIG. 2. B_z vs time measured at different locations of the Hall probes. Probe number 2 (p No. 2) is located near the center. Probe number 10 (p No. 10) is close to the edge of the sample.

Bean like model for an infinite strip in a perpendicular field.¹¹ This one parameter fit allows determination of the current density j , and thus the calculation of the in plane component B_x of the induction, as shown by the dashed curve in Fig. 1. Signatures of demagnetization effects typical for such a thin sample¹¹ are clearly observed. Specifically, B_z at the sample edge is not equal to the externally applied field H , because of the sample contribution to B_z . This contribution has a different sign at the edge and at the center, and there exist a contour inside the sample where $B = H$ exactly. This contour is sometimes referred to as a ‘‘neutral line’’.¹² In the flux creep process, the induction increases at the sample center and it decreases at the sample edge. At the neutral line where $B = H$, the induction does not change with time. This is illustrated in Fig. 2 which shows B_z as a function of time at different locations in the sample. Evidently, the relaxation rate $\partial B_z / \partial(\ln t)$ is maximum near the center (probe No. 1) and decreases toward the neutral line (probe No. 8). Beyond the neutral line and toward the edge of the sample the induction *decreases* with time, exhibiting a *negative* relaxation rate. These results demonstrate the nonuniformity of the local relaxation, thus questioning the meaning of global measurements in which all contributions are integrated.

Using the raw $B_z(x, t)$ data, we calculate the local relaxation rates $\partial B_z(x, t) / \partial t$, and then numerically integrate $\partial B_z(x, t) / \partial t$ in order to determine the flux current density $D(x, t)$ according to Eq. (4):

$$D(x, t) = - \int_0^x \frac{\partial B_z(x, t)}{\partial t} dx. \quad (7)$$

In Eq. (7), $x = 0$, is the center of the sample where $D \equiv 0$. In Fig. 3, we plot the flux line current density D as a function of x at different times. Note that according to Eqs. (7) and (4), the slope of $D(x)$ is related to the rate of change of B_z with time. The latter is maximum at the center and it drops to zero at the neutral line, see Fig. 2. The behavior of D is thus consistent with this picture: it has an inflection point at the center and a maximum at the neutral line. Experimentally,

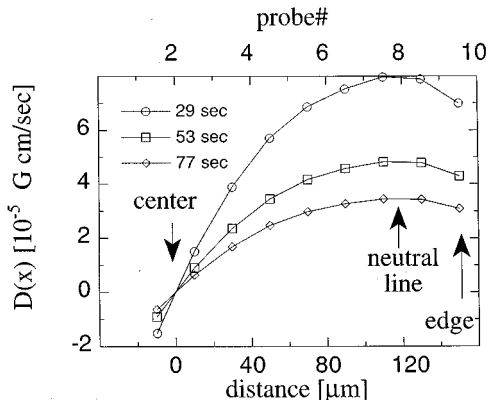


FIG. 3. Flux current density D as a function of the distance from the edge, measured at the indicated times. Note the maximum in D at the neutral line.

the maximum is clearly observed here for the first time because the neutral line is quite far from the edge due to the large aspect ratio of the sample.

From the experimental data on the flux line current density D , it is easy to derive the flux line velocity v , using the definition $D = vB$. Typical data for v as a function of x are shown in Fig. 4. The behavior of v is similar to that of D , it is small near the center, and has a maximum near the neutral line. It should be noted that the time dependence of v is hyperbolic; in the logarithmic approximation (6) one obtains $v = v_0(t_0/t)$. The parameter v_0 , being proportional to the current density j , depends only logarithmically on the time t .

Using the $v(x, t)$ data, we obtain the activation energy $U(x, t)$ according to Eq. (6) as explained above. Typical results of U/kT are shown in Fig. 5. The figure shows a linear dependence of U/kT on $\ln(t)$ with a slope of 1 in the long-time limit in accordance with the logarithmic solution

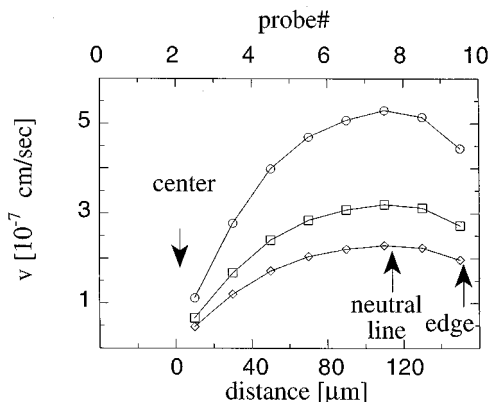


FIG. 4. Flux line velocity v as a function of the distance from the edge, measured at the indicated times.

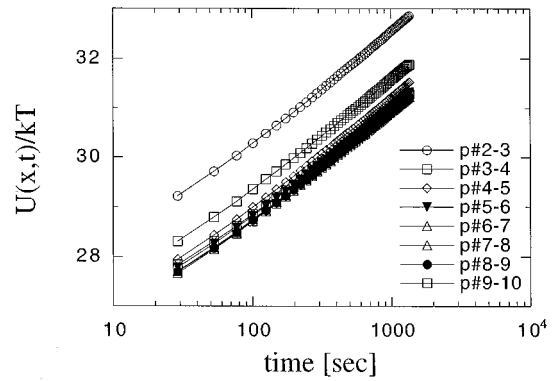


FIG. 5. Local activation energy U/kT vs time for different probes.

$U = kT \ln(t/t_0)$ of the continuity equation.¹ The increase of U with time is a reflection of the increase of U with the decrease of the current density j .

In conclusion, we investigated thermally activated flux creep in a *thin* NCCO crystal using a novel Hall sensor array technique. Our unique method allows a direct determination of the flux creep parameters as a function of time and position, thus giving a complete picture of the relaxation process within the sample. It can serve as an effective tool in investigating various phenomena such as collective (elastic) and plastic creep, surface barriers, and “fishtail” effects.⁴

We thank H. Shtrikman for growing the GaAs heterostructures, and acknowledge useful discussions with L. Burlachkov, V. Vinokur, and V. B. Geshkenbein. This work was supported by the Israel Science Foundation administered by the Israeli Academy of Science and Humanities, and the Heinrich Hertz Minerva Center for High Temperature Superconductivity. Y. Y. acknowledges support from the DG XII, Commission of the European Communities. Y. Y. and E. Z. acknowledge support from the USA-Israel Binational Science Foundation. A. S. and E. Z. acknowledge support from the France-Israel Cooperation program AFIRST. J. L. P. and R. L. G. acknowledge support from NSF Grant No. DMR-9510475.

¹G. Blatter *et al.*, Rev. Mod. Phys. **66**, 1125 (1994).

²Y. Yeshurun, A. P. Malozemoff, and A. Shaulov, Rev. Mod. Phys. (in press).

³Y. Abulafia *et al.*, Phys. Rev. Lett. **75**, 2404 (1995).

⁴Y. Abulafia *et al.*, Phys. Rev. Lett. **77**, 1596 (1996).

⁵Y. Abulafia, A. Shaulov, Y. Wolfus, R. Prozorov, L. Burlachkov, D. Majer, E. Zeldov, V. M. Vinokur, and Y. Yeshurun, Proceedings of the International Conference on Physics and Chemistry of Molecular and Oxide Superconductors, Karlsruhe, Germany, August 1996 (unpublished).

⁶F. Zuo, S. Khizroev, X. Jiang, J. L. Peng, and R. L. Greene, J. Appl. Phys. **76**, 6953 (1994).

⁷D. Giller *et al.* (unpublished).

⁸M. V. Feigel'man, V. B. Geshkenbein, and V. M. Vinokur, Phys. Rev. B **43**, 63 (1991).

⁹N.-C. Yeh *et al.*, Phys. Rev. B **48**, 9861 (1993).

¹⁰J. L. Peng, Z. Y. Li, and R. L. Greene, Physica C **177**, 79 (1991).

¹¹E. H. Brandt, Phys. Rev. B **49**, 9024 (1994); E. Zeldov *et al.*, Phys. Rev. B **49**, 9802 (1994).

¹²T. Schuster, H. Kuhn, and E. H. Brandt, Phys. Rev. B **51**, 697 (1995).